Available online at www.sciencedirect.com
ScienceDirect
Thin Solid Films 516 (2008) 4613–4619
www.elsevier.com/locate/tsf

Fabrication of thin film dye sensitized solar cells with solar to electric power conversion efficiency over 10%

Seigo Ito *, Takurou N. Murakami [1], Pascal Comte [1], Paul Liska [1], Carole Grätzel [1], Mohammad K. Nazeeruddin [1], Michael Grätzel *

Laboratoire de Photonique et Interfaces, Institut des Sciences et Ingénierie Chimiques, École Polytechnique Fédérale de Lausanne (EPFL), Station 6, CH-1015, Lausanne, Switzerland

Available online 14 June 2007

Abstract

Techniques of TiO_2 film fabrication for dye-sensitized solar cells having a conversion efficiency of global air mass 1.5 (AM 1.5, 1000 W/m^2) solar light to electric power over 10% are reported. Newly implemented fabrication technologies consist of pre-treatment of the working photoelectrode by $TiCl_4$, variations in layer thickness of the transparent nanocrystalline-TiO_2 and applying a topcoat light-scattering layer as well as the adhesion of an anti-reflecting film to the electrode's surface. $TiCl_4$ treatments induce improvements in the adhesion and mechanical strength of the nanocrystalline TiO_2 layer. Optimization of the thickness of the TiO_2 layer, acting as the working electrode, affects both the photocurrent and the photovoltage of the devices. Covering of the TiO_2 photoanode by an anti-reflecting film results in enhancement of the photocurrent. Each of these components of film fabrication exerts a significant influence on the overall photovoltaic parameters of the devices resulting in improvements in the net energy conversion performance.
© 2007 Elsevier B.V. All rights reserved.

Keywords: Dye-sensitized solar cells; Porous TiO_2 film; Screen printing; High conversion efficiency; Reproducibility; $TiCl_4$ treatment; Light-scattering layer; Anti-reflecting film

1. Introduction

Dye-sensitized solar cells (DSC) show great promise as an inexpensive alternative to conventional p–n junction solar cells. Investigations into the various factors influencing the photovoltaic efficiency in this novel approach have recently been intensified [1–4]. Highly efficient photovoltaic conversions, combined with ease of manufacturing and low production costs, make the DSC technology an attractive approach for large-scale solar energy conversion [5]. For the optimization of the DSC components, i.e., the oxide semiconductor, the sensitizer and the electrolyte, exactitude in reporting the experimental procedures used is indispensable in order to compare the data between the many different laboratories active in this field.

Amongst the concepts fundamental to the development of the dye-sensitized solar cell is the association of a highly porous nanocrystalline TiO_2 film (affording a large inherent adsorptive surface area), enhanced in recent designs by a light-scattering topcoat, with a high molar extinction coefficient dye as sensitizer to form the working electrode of the solar cell. Techniques in TiO_2 film fabrication are, thus, a very important aspect in the production of highly efficient DSCs. TiO_2 film preparation utilizes the techniques of screen-printing for the nanocrystalline and submicron-crystalline-TiO_2 film layers as well as a chemical bath deposition for the $TiCl_4$ treatment [6]. A photon-trapping effect is induced by the use of the so-called "double layer" [7], i.e., the combination of a transparent nanocrystalline TiO_2 film with a microcrystalline light-scattering layer, in conjunction with an anti-reflecting film (ARF), thus, enhancing the incident photon-to-electricity conversion efficiency (IPCE), also referred to as the "external quantum efficiency".

This manuscript describes the methodical fabrication of the TiO_2 electrodes exploring the optimal cell design, while analyzing the influence of various technical procedures on the photovoltaic

* Corresponding authors. Tel.: +41 21 693 3112; fax: +41 21 693 6100.
E-mail address: michael.graetzel@epfl.ch (M. Grätzel).
[1] Tel.: +41 21 693 3112; fax: +41 21 693 6100.

0040-6090/$ - see front matter © 2007 Elsevier B.V. All rights reserved.
doi:10.1016/j.tsf.2007.05.090

performance of highly efficient DSC. A detailed procedure is presented for fabrication of cells showing reproducible conversion efficiencies over 10% under standard reporting conditions.

2. Experimental details

2.1. Materials

4-tert-butylpyridine (Aldrich), acetonitrile (Fluka), and valeronitrile (Fluka) were purified by vacuum distillation. Guanidinium thiocyanate (Aldrich) and H_2PtCl_6 (Fluka) were used as received. H_2O was purified by distillation and filtration (Milli-Q). $TiCl_4$ (Fluka) was diluted with water to 2 M at 0 °C to make a stock solution, which was kept in a freezer and freshly diluted to 40 mM with water for each $TiCl_4$ treatment of the FTO coated glass plates. Iodine (99.999%), (Superpur®, Merck) was used as received. 1-butyl-3-methyl imidazolium iodide (BMII) was prepared according to the literature method [8].

2.2. Preparation of TiO_2 screen-printing pastes

Two types of TiO_2 pastes yielding nanocrystalline-TiO_2 (20 nm, paste A) and microcrystalline-TiO_2 (400 nm, paste B) particles were prepared, forming respectively the transparent and the light-scattering layers of the photoanode. Scheme 1 depicts the stepwise preparation procedures for the paste (A) containing nanocrystalline-TiO_2 (20 nm) particles.

2.2.1. 20 nm particle sized TiO_2 colloid: preparation and characterization

An amount of 12 g (0.2 moles) of acetic acid was added all at once to 58.6 gm (0.2 moles) of titanium iso-propoxide under stirring at room temperature. The modified precursor was stirred for about 15 min and poured into 290 ml water as quickly as possible while vigorously stirring (700 rpm). A white precipitate was instantaneously formed. One hour of stirring was required to achieve a complete hydrolysis reaction. After adding a quantity of 4 ml of concentrated nitric acid, the mixture was heated from room temperature to 80 °C within 40 min and peptized for 75 min. Water was then added to the cooling liquid mixture to adjust the volume to a final 370 ml. The resultant mixture was kept in a 570 ml titanium autoclave and heated at 250 °C for 12 h. Following this step, 2.4 ml of 65% nitric acid was added and the dispersion was treated with a 200 W ultrasonic titanium probe at a frequency of 30 pulses every 2 s. The resultant colloidal solution was concentrated with a rotary-evaporator to contain 13 wt.% TiO_2. Finally, it was triply centrifuged to remove nitric acid and washed with ethanol three times to produce a white precipitate containing 40 wt.% TiO_2 in ethanol and only trace amounts of water.

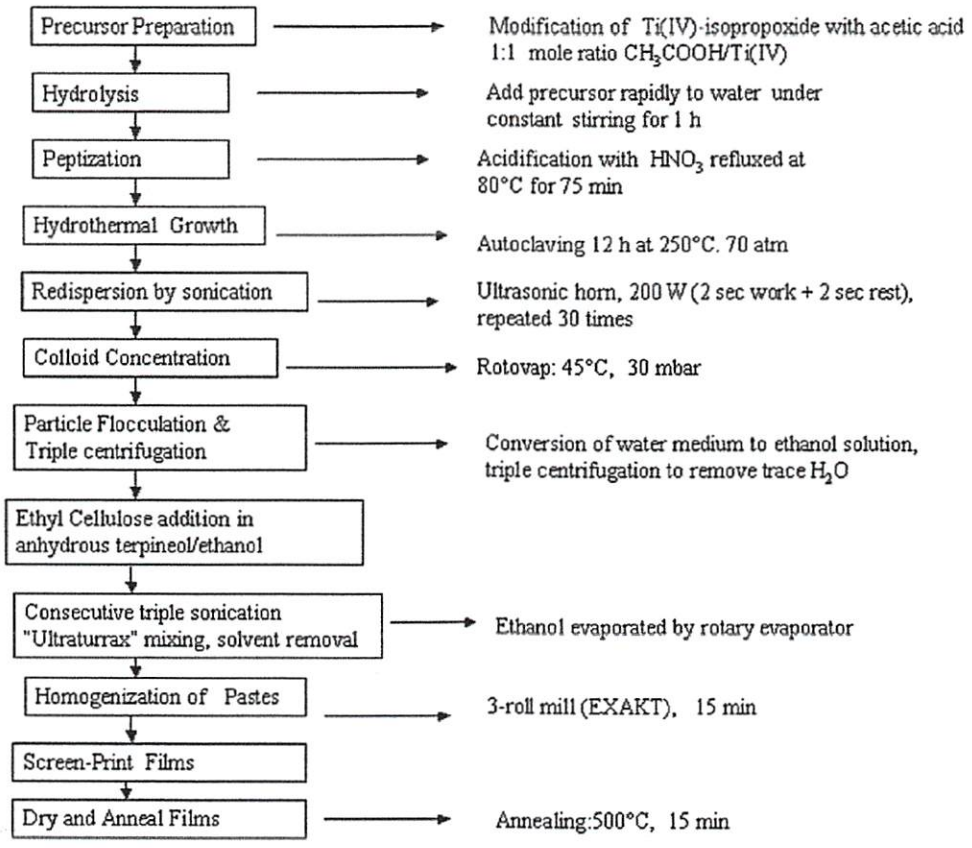

Scheme 1. Flow diagram depicting TiO_2 colloid and paste used in screen-printing technique for DSC production.

2.2.2. Preparation of screen-printing pastes

Two kinds of pure ethyl cellulose (EC) powders, i.e., EC (5–15 mPas, #46070, Fluka) and EC (30–50 mPas, #46080, Fluka) were dissolved prior to usage in ethanol to yield 10 wt.% solutions. 45 g of EC (5–15, #46070) and 35 g of EC (30–50), #46080) of these 10 wt.% ethanolic mixtures were added to a round bottomed rotavap flask containing 16 g pure TiO2 (obtained from previously prepared precipitate) and 64.9 g of terpineol (anhydrous, #86480, Fluka) and diluted with 80 ml of ethanol to obtain a final total volume of 280 ml. This mixture was then sonicated using an ultrasonic horn (Sonics & Materials, Inc), alternating stirring, with a hand mixer (Ultraturrax, IKA), and sonication, for three consecutive times. Ethanol and water were removed from these TiO_2/ethyl cellulose solutions by rotary-evaporator (initial temperature 40 °C and pressure 120 mbar subsequently reduced to a final pressure of 10 mbar at 40 °C). The final formulations of the pastes were made with a three-roll mill (M-50, EXAKT, Germany). The final screen-printing pastes correspond to 18 wt.% Ti02, 9 wt.% ethyl cellulose and 73 wt.% terpineol (paste A).

For the paste used in the light-scattering layers (paste B), 10 nm TiO_2 particles which were obtained following the peptization step (particle size is determined at this stage of fabrication) and in a procedure analogous to those of 20 nm TiO_2 outlined in Scheme 1, were mixed with 400 nm TiO_2 colloidal solution (CCIC, Japan) to give a final paste formulation of 28.6% 400 nm-sized TiO_2, 2.9% 10-nm-sized TiO_2 and 7.2% ethyl cellulose [EC 30–50 (#46080)] in terpineol.

2.3. Synthesis of ruthenium sensitizer

The synthesis of *cis*-di(thiocyanato)-*N*-*N*′-bis(2,2′-bipyridyl-4-carboxylic acid-4′-tetrabutylammonium carboxylate) ruthenium (II) (N-719) was reported previously [9]. The chromatographic purification of N-719 was carried out three times on a column of Sephadex LH-20 using the literature procedure [10]. The N-719 complex was dissolved in water containing two equivalents of tetrabutylammonium hydroxide. The concentrated solution was filtered through a sintered glass crucible and charged onto a Sephadex LH-20 column, which was prepared in water. The adsorbed complex was eluted using water. The main band was collected, and the solution pH was lowered to 4.3 using 0.02 M HNO_3 acid. The titration was carried out slowly over a period of 3 h. The solution was then kept at −20 °C for 15 h. After allowing the flask to return to ambient temperature (25 °C), the precipitated complex was collected on a glass frit and air-dried. The same purification procedure was repeated three times to get pure N-bonded isomer complex.

2.4. Fabrication of porous-TiO_2 electrodes

In order to obtain an efficient and reproducible photovoltaic DSC performance, surface contamination by iron cations should be avoided, because these ions or iron oxides formed during the subsequent sintering of the TiO_2 layer enhance charge recombination in photocells [11,12]. Indeed we found that deposition of Fe^{3+} by application of an aqueous $FeCl_3$ solution to the TiO_2 electrode quenches the dye-sensitized photocurrent (J_{sc}) effectively. The J_{sc} decreased by 30% upon addition of 400 ppm Fe_2O_3 [13]. In order to exclude iron contamination the equipment used during the preparation of mesoscopic TiO_2 was made of plastic, titanium or glass, and was washed with an acidic solution prior to use. Plastic tweezers and spatulas were employed throughout. The treatment as mentioned below with solutions of 0.1 M HCl in ethanol or $TiCl_4$ (aqueous) had the effect to remove the iron contamination source.

As shown in Scheme 2, to prepare the DSC working electrodes, the FTO glass used as current collector (Solar 4 mm thickness, 10Ω/□, Nippon Sheet Glass, Japan) was first cleaned in a detergent solution using an ultrasonic bath for 15 min, and then rinsed with water and ethanol. After treatment in a UV-O_3 system (Model No. 256–220, Jelight Company, Inc.) for 18 min, the FTO glass plates were immersed into a 40 mM aqueous $TiCl_4$ solution at 70 °C for 30 min and washed with water and ethanol. A layer of paste A was coated on the FTO glass plates by screen-printing (90T, Estal Mono, Schweiz. Seidengazefabrik, AG, Thal), kept in a clean box for 3 min so that the paste can relax to reduce the surface irregularity and then dried for 6 min at 125 °C. However, this "leveling" (i.e., reduction in surface irregularity) time must be controlled visually by the experimentalist since the speed at which this leveling occurs depends on the viscosity of each paste employed. The screen characteristics are as follows: material, polyester; mesh count, 90T mesh/cm (or 230T mesh/inch); mesh opening, 60 μm; thread diameter, 50 μm; open surface, 29.8%; fabric thickness, 83 μm; theoretical paste volume, 24.5 cm^3/m^2; K/KS volume, 17.0 cm^3/m^2; weight, 48 g/m^2. This screen-printing procedure with paste A (coating, storing and drying) was repeated to get an appropriate thickness of 12–14 μm for the working electrode. After drying the (paste A) films at 125 °C, two layers of paste B were deposited by screen-printing, resulting in a light-scattering TiO_2 film containing 400 nm sized anatase particles of 4–5 μm thickness. The electrodes coated with the TiO_2 pastes were gradually heated under an airflow at 325 °C for 5 min, at 375 °C for 5 min, and at 450 °C for 15 min, and finally, at 500 °C for 15 min.

The TiO_2 "double-layer" film thus produced is once again treated with 40 mM $TiCl_4$ solution, as described previously, then rinsed with water and ethanol and sintered at 500 °C for 30 min. After cooling to 80 °C, the TiO_2 electrode was immersed into a 0.5 mM N-719 dye solution in a mixture of acetonitrile and tert-butyl alcohol (volume ratio, 1:1) and kept at room temperature for 20–24 h to assure complete sensitizer uptake.

2.5. Preparation of counter Pt-electrodes

To prepare the counter electrode, a hole (1-mm diameter) was drilled in the FTO glass (LOF Industries, TEC 15 Ω/□, 2.2 mm thickness) by sandblasting. The perforated sheet was washed with H_2O as well as with a 0.1 M HCl solution in ethanol and cleaned by ultrasound in an acetone bath for 10 min. After removing residual organic contaminants by heating in air for 15 min at 400 °C, the Pt catalyst was deposited on the FTO glass by coating with a drop of H_2PtCl_6 solution (2 mg Pt in 1 ml ethanol) with repetition of the heat treatment at 400 °C for 15 min.

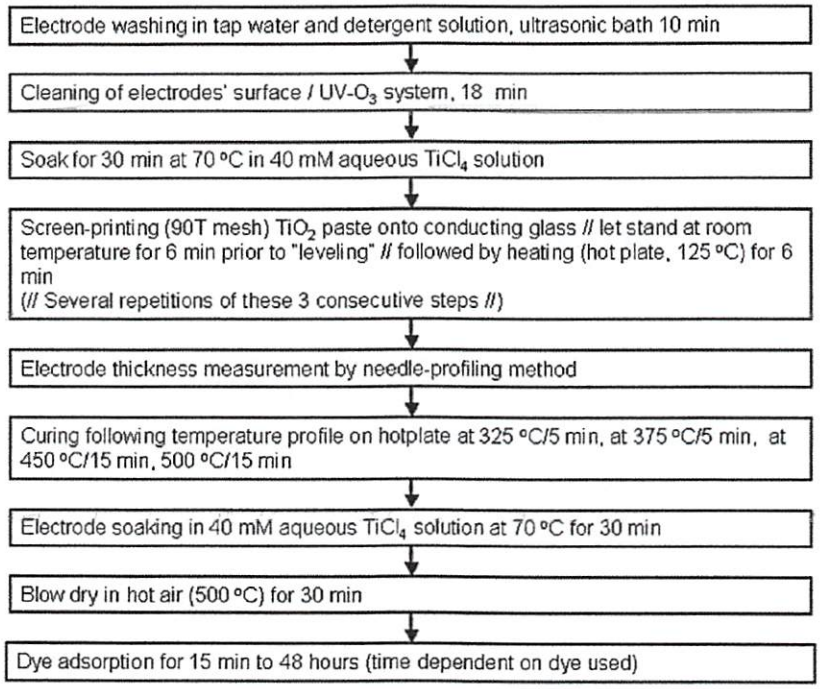

Scheme 2. Schematic representation for fabrication of dye-sensitized-TiO_2 electrodes.

2.6. Electrolyte

The electrolyte employed was a solution of 0.6 M BMII, 0.03 M I_2, 0.10 M guanidinium thiocyanate and 0.5 M 4-tert-butylpyridine in a mixture of acetonitrile and valeronitrile (volume ratio, 85:15).

2.7. DSC assemblage

The dye-covered TiO_2 electrode and Pt-counter electrode were assembled into a sandwich type cell (Fig. 1) and sealed with a hot-melt gasket of 25 μm thickness made of the ionomer Surlyn 1702 (Dupont). The size of the TiO_2 electrodes used was 0.16 cm^2 (i.e., 4 mm × 4 mm). The aperture of the Surlyn frame was 2 mm larger than that of the TiO_2 area and its width was 1 mm. The hole in the counter electrode was sealed by a film of Bynel using a hot iron bar (protectively covered by a fluorine polymer film). A hole was then made in the film of Bynel by a needle. A drop of the electrolyte was put on the hole in the back of the counter electrode. It was introduced into the cell via vacuum backfilling. The cell was placed in a small vacuum chamber to remove inside air. Exposing it again to ambient pressure causes the electrolyte to be driven into the cell. Finally, the hole was sealed using a hot-melt ionomer film (Bynel 4702, 35 μm thickness, Dupont) and a cover glass (0.1 mm thickness).

In order to have a good electrical contact for the connections to the measurement set-up, the edge of the FTO outside of the cell was roughened slightly with sandpaper or a file. A solder (Cerasolza, Asahi Glass) was applied on each side of the FTO electrodes. The position of the solder was 1 mm away from the edge of the Surlyn gasket and hence 4 mm away from the side of the photoactive TiO_2 layer.

Light reflection losses were eliminated using a self-adhesive fluorinated polymer film (Arktop, Asahi Glass) that served at the same time as a 380 nm UV cut-off filter Masks made of black plastic tape were attached on the Arktop filter to reduce scattered light.

2.8. Photovoltaic measurements

Photovoltaic measurements employed an AM 1.5 solar simulator equipped with a 450 W xenon lamp (Model No. 81172, Oriel). The power of the simulated light was calibrated

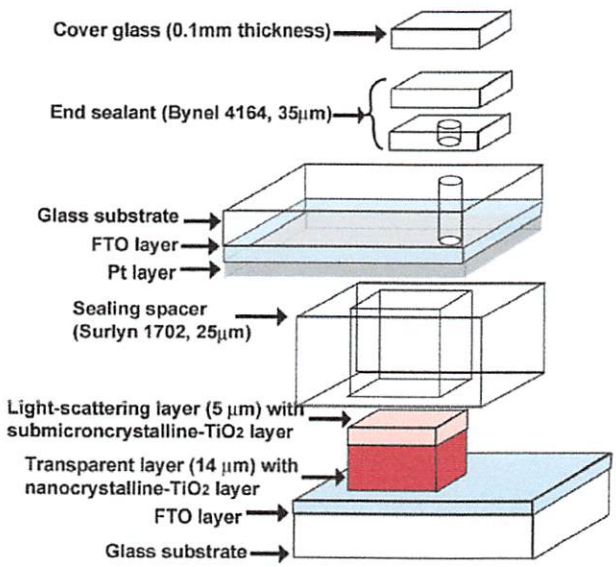

Fig. 1. Configuration of the dye sensitized solar cells.

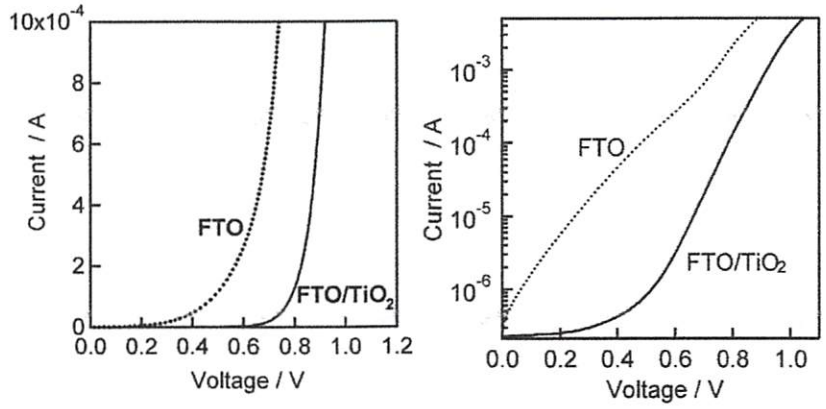

Fig. 2. Dark I–V curves of smooth electrodes measured in the absence of Ru-dye sensitizer. Left graph: linear current scale: dotted line, bare FTO; solid line, FTO covered with TiO_2 layer. Right graph: logarithmic current scale; FTO (bare) [dotted line], FTO/TiO_2 [solid line]. Compact layer TiO_2 on FTO was made using a dual $TiCl_4$ treatment. Sandwich cell configuration as depicted in Fig. 1.

to 100 MW/cm^2 by using a reference Si photodiode equipped with an IR-cutoff filter (KG-3, Schott) in order to reduce the mismatch between the simulated light and AM 1.5 (in the region of 350–750 nm) to less than 2% [14,15] with measurements verified at two solar-energy institutes [ISE (Germany), NREL (USA)]. I–V curves were obtained by applying an external bias to the cell and measuring the generated photocurrent with a Keithley model 2400 digital source meter. The voltage step and delay time of photocurrent were 10 mV and 40 ms, respectively.

3. Results and discussion

3.1. $TiCl_4$ treatments

Two consecutive $TiCl_4$ treatments were performed when preparing the TiO_2 photoanodes for dye sensitized solar cells, one prior to and one following the screen printing of the mesoscopic (porous)-TiO_2 films (Scheme 2). The initial $TiCl_4$ treatment influences positively the TiO_2 working electrode in two manners, firstly through enhancing the bonding strength between the FTO substrate and the porous-TiO_2 layer, and secondly, by blocking the charge recombination between electrons emanating from the FTO and the I_3^- ions present in the I^-/I_3^- redox couple. Frank et al. [16] concluded from Intensity-Modulated Infrared Spectroscopy (IMIS) analysis that recombination occurs predominantly in the region of the FTO substrate rather than across the depth of the TiO_2 film, underlining the utility of applying a TiO_2 compact "under" layer to the FTO glass surface. The second $TiCl_4$ treatment has itself been shown to enhance the surface roughness factor and necking of the TiO_2 particles thus augmenting dye adsorption and resulting in higher photocurrent [6].

Fig. 2 exhibits the dark current–voltage characteristics of two types of electrode surfaces, one consisting merely of FTO conducting glass with the other being $TiCl_4$ treated FTO glass. The onset of the dark current emanating from the non-treated FTO substrate occurs at low forward bias as is clearly discernible on the right diagram where the current is plotted on a logarithmic scale. $TiCl_4$ treatment is shown, however, to suppress the dark current, shifting its onset by several hundred millivolts. This can be attributed to the fact that the SnO_2 is highly doped and its conduction band edge is positively shifted by about 0.5 V with respect to that of TiO_2 resulting in a much higher electron density in the FTO glass within the investigated potential range. The suppression of dark current following compact TiO_2 film formation is indicative of the tri-iodide reduction being enhanced at any exposed part of the FTO substrate in addition to occurring at the TiO_2 film itself or at the interface of the dye sensitized-TiO_2 and the electrolyte employed in cell fabrication.

Table 1 shows the influence of $TiCl_4$ chemical bath deposition on the characteristics of nanocrystalline-TiO_2 layers which have been treated versus those layers prepared according to the original procedure [6] used in nanocrystalline-TiO_2 film formation. Although the specific surface area decreased by 7.9% following the $TiCl_4$ treatment, the overall weight of TiO_2 increased by 28.1% leading to an increase in the TiO_2 roughness factor. The augmentation in the roughness factor leads to an absorbance increase of 15.7%. The increase of particle diameter (by 1.9 nm) following the $TiCl_4$ treatment implies the generation of an

Table 1
Characteristics of nanaocrystalline TiO_2 layers illustrating the effects of the $TiCl_4$ treatments [1]

Film characteristics	Electrode description	
	Nano-TiO_2	$TiCl_4$-treated nano-TiO_2
Average pore diameter/nm	20.2	18.3
Specific surface area/m^{2}g^{-1}	86.0	79.7
TiO_2 weight[a]/mg cm^{-2}μm^{-1}	0.135±0.003	0.173±0.003
Roughness factor[b]/μm^{-1}	116±3	138±2
Absorbance at 540[c]nm/μm^{-1}	0.159±0.05	0.184±0.06

The optical reference background was obtained using an identical TiO_2 electrode after desorption of N-719 by soaking in a 0.1 M solution of tert-butylammonium hydroxide in acetonitrile. A cover glass was attached to the TiO_2 layer surface and the pores in nanocrystalline TiO_2 layers were filled with butoxyacetonitrile to decrease the light-scattering effect. Note: the last three characteristics tabulated are "per μm" electrode thickness.

[a] The weight-measurement sample area was 16 cm^2 for a 15 μm thickness.

[b] Roughness factor was obtained by multiplying the specific surface area and TiO_2 weight.

[c] Absorbance measurements were performed with a N719-covered nanocrystalline TiO_2 layer at 540 nm.

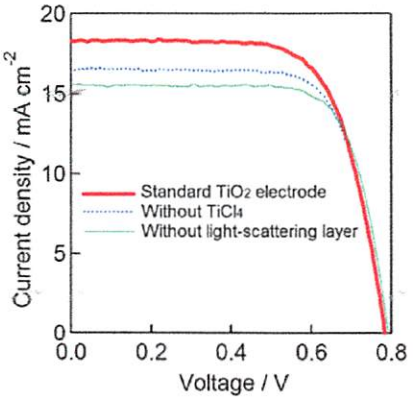

Fig. 3. I–V curves comparing TiO_2 electrodes produced using the standard procedure [6] (thick line), without $TiCl_4$ treatment (dotted line), and without a light-scattering layer (thin line). Cell characteristics described in text. The total active area of the cell was 0.25 cm^2; the illuminated part corresponding to the aperture area of the black mask was 0.16 cm^2. The V_{oc} loss due to partial illumination of the active area is about 20–30 mV depending on J_{sc}. Photovoltaic characteristics on TiO_2 electrodes were: standard procedure: J_{sc}= 18.2 mA cm^{-2}, V_{oc}=789 mV, FF=0.704 and η=10.1%; no $TiCl_4$ treatment, J_{sc}=16.6 mA cm^{-2}, V_{oc}=778 mV, FF=0.731 and η=9.4%; no light-scattering layer, J_{sc}=15.6 mA cm^{-2}, V_{oc}=791 mV, FF=0.740 and η=9.12%.

additional TiO_2 layer (of approximately 1 nm thickness) on the surface of the nanocrystalline-TiO_2 film present in the porous layer. The photocurrent and the conversion efficiency increased by 9.6% and 8.0%, respectively, attributed to the increase of the roughness factor, with its resultant enhanced dye adsorbance, leading to DSC conversion efficiencies of more than 10%.

3.2. Effect of the light-scattering TiO_2 (anatase) layer

A photon-trapping system, the so-called "double-layer" (i.e., TiO_2 films consisting of transparent nanocrystalline and microcrystalline light-scattering anatase particles), was used for DSC photocurrent enhancement. Fig. 3 exhibits the photovoltaic improvements engendered by using the double-layer TiO_2 films. The total active cell area was 0.25 cm^2 and the cell area illuminated through the aperture of the mask was 0.16 cm^2, respectively. With no light-scattering layer present the photovoltaic parameters measured were J_{sc}=15.6 $mAcm^{-2}$, V_{oc}= 791 mV, FF=0.740 and η=9.12%. Upon addition of the light-scattering layer, these same photovoltaic characteristics displayed an enhancement, i.e., J_{sc}=18.2 $mAcm^{-2}$, V_{oc}=785 mV, FF=0.704 and η=10.1%.

The light-scattering layer has been shown to act not only as a photon-trapping system but to be equally active in photovoltaic generation itself [17]. Cell efficiencies measured were 5% in dye sensitized solar cells using only the light-scattering TiO_2 layer.

Losses of approximately 4% on the glass substrate due to reflection of incident light in DSC can be partially circumvented by adding an anti-reflecting film, which acts simultaneously as a 380 nm UV cut-off filter. Fig. 4 compares the incident photon-to-electron conversion efficiency (IPCE), or "external quantum efficiency" of a cell with and without the anti-reflecting layer.

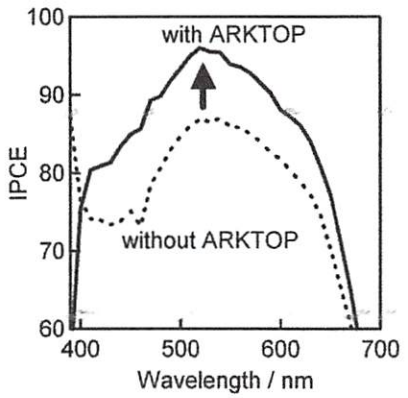

Fig. 4. IPCE of DSC with and without adhesion of ARKTOP anti-reflecting film.

3.3. Impact of nanocrystalline-TiO_2 layer thicknesses on photovoltaic performance

Variation in thickness of the nanocrystalline-TiO_2 layer is a crucial factor in optimizing photovoltaic performances of DSC. Although precise measurements of the exact layer thickness is difficult to perform following formation of the "double-layer" electrode, the nanocrystalline-TiO_2 layer can be measured prior to sintering using a surface profiler. In order to facilitate depth estimations and to make useful projections of the final thickness of the nanocrystalline-TiO_2 layer comprised in the "double layer" electrode following sintering, a calibration curve was made. The ratio "before sintering"/"after sintering", described by a linear relationship going through the origin, yields a shrinkage factor of slightly under unity (i.e., 0.942) for 20 nm TiO_2 sized particulate films. By using this calibration line, a relationship between nanocrystalline-TiO_2 film thickness and the resultant DSC conversion efficiency can be obtained, the optimum film thickness to produce highly efficient DSC being 12–14 μm (with the addition of an adhered ARF), as shown in Fig. 5.

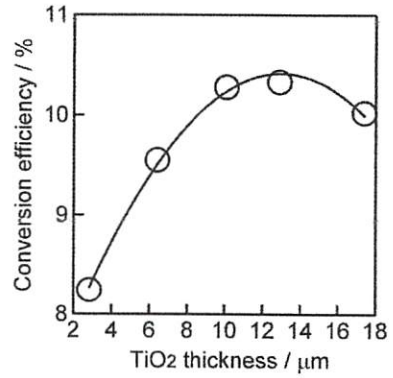

Fig. 5. Photoconversion efficiency as a function of nanocrystalline TiO_2 layer thickness. Illuminated-TiO_2 and aperture areas of cells are 0.16 cm^2 and 0.25 cm^2, respectively [18].

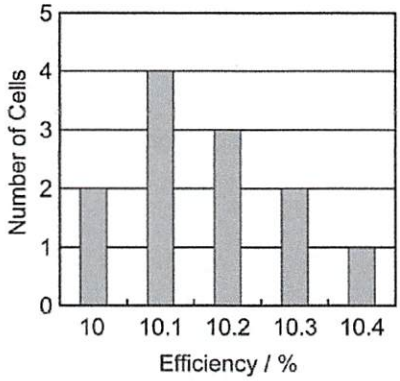

Fig. 6. Histogram depicting reproducibility of DSC conversion efficiencies. Reported values of 12 DSC devices produced with a 24 hour time period.

3.4. Reproducibility of DSC fabrication

Fig. 6 depicts a histogram showing the performance statistics of twelve devices produced within 24 hours of each other by following the procedure described above, optimizing cell performance parameters through $TiCl_4$ treatments, nanocrystalline-TiO_2 layer thickness selection as well as by use of an anti-reflecting film (Arktop). Conversion efficiencies greater than 10% were obtained with all devices, the average being 10.2± 0.2%. This statistical graph shows convincingly the excellent reproducibility of the method elaborated here for the fabrication of highly efficient dye sensitized solar cells.

4. Conclusions

The present study systematically outlines the step-by-step procedures to follow in producing screen-printing pastes used to form both the transparent and light-scattering layers of TiO_2 electrodes used in DSC devices. A methodological approach to the actual TiO_2 electrode fabrication is likewise outlined complementing other systematic studies of experimental procedures [18]. Adhesion of an anti-reflecting film (ARF) is seen to enhance the IPCE or "external quantum efficiency" of the devices to reach up to 94% at wavelengths close to the absorption maximum of the sensitizer. Optimization of the nanocrystalline-TiO_2 layer thickness (12–14 μm) is shown to play a crucial role in cell design.

The protocol established here should assist researchers involved in the fabrication and characterization of small DSC laboratory cells as well as in the production of commercialized panels. Combination of all of these "state of the arts" procedures renders the production of reproducible, highly efficient (>10%) dye-sensitized solar cells easily attainable.

Acknowledgement

This work was supported by a grant from the Swiss Federal Energy Office (OFEN). Aid in manuscript preparation by Dr. Daibin Kuang and experimental assistance by Drs. Shaik Zakeeruddin and Peter Pechy is gratefully acknowledged.

References

[1] B. O'Regan, M. Grätzel, Nature 335 (1991) 737.
[2] M. Grätzel, Nature 414 (2001) 338.
[3] A. Hagfeldt, M. Grätzel, Acc. Chem. Res. 33 (2000) 269.
[4] U. Bach, D. Lupo, P. Comte, J.E. Moser, F. Weissörtel, J. Salbeck, H. Spreitzert, M. Grätzel, Nature 395 (1998) 544.
[5] G. Smestad, Sol. Energy Mater. Sol. Cells 32 (1994) 259.
[6] S. Ito, P. Liska, R. Charvet, P. Comte, P. Péchy, Md. K. Nazeeruddin, S.M. Zakeeruddin, M. Grätzel, Chem. Commun. (2005) 4351.
[7] P. Wang, S.M. Zakeeruddin, P. Comte, R. Charvet, R. Humphry-Baker, M. Grätzel, J. Phys. Chem., B 107 (2003) 14336.
[8] P. Bonhôte, A.P. Dias, M. Armand, N. Papageorgiou, K. Kalyanasundaram, M. Grätzel, Inorg. Chem. 35 (1996) 1168.
[9] Md. K. Nazeeruddin, S.M. Zakeeruddin, R. Humphry-Baker, M. Jirousek, P. Liska, N. Vlachopoulos, V. Shklover, Christian-H. Fischer, M. Grätzel, Inorg. Chem. 38 (1999) 6298.
[10] Md. K. Nazeeruddin, F. De Angelis, S. Fantacci, A. Selloni, G. Viscardi, P. Liska, S. Ito, B. Takeru, M. Gratzel, J. Am. Chem. Soc. 127 (2005) 16835.
[11] N.J. Cherepy, D.B. Liston, J.A. Lovejoy, H. Deng, J.Z. Zhang, J. Phys. Chem., B 102 (1998) 770.
[12] B.A. Gregg, F. Pichot, S. Ferrere, C.L. Fields, J. Phys. Chem., B 105 (2001) 1422.
[13] A. Kay, PhD Thesis, Ecole Polytechnique Fédérale de Lausanne, Switzerland (1994).
[14] M.K. Nazeeruddin, P. Péchy, T. Renouard, S.M. Zakeeruddin, R. Humphry-Baker, P. Comte, P. Liska, L. Cevey, E. Costa, V. Shklover, L. Spiccia, G.B. Deacon, C.A. Bignozzi, M. Grätzel, J. Am. Chem. Soc. 123 (2001) 1613.
[15] S. Ito, H. Matsui, K. Okada, S. Kusano, T. Kitamura, Y. Wada, S. Yanagida, Sol. Energy Mater. Sol. Cells 82 (2004) 421.
[16] K. Zhu, E.A. Schiff, N.-G. Park, J. Van de Lagemaat, A.J. Frank, Appl. Phys. Lett. 80 (2002) 685.
[17] Z. Zhang, S. Ito, B. O'Regan, D. Kunag, S.M. Zakeeruddin, P. Liska, R. Charvet, P. Comte, Md. K. Nazeeruddin, P. Péchy, R. Humphry-Baker, T. Koyanagi, T. Mizuno, M. Grätzel, Z. Phys. Chem. 221 (2007) 319.
[18] S. Ito, Md. K. Nazeeruddin, P. Liska, P. Comte, R. Charvet, P. Péchy, M. Jirousek, A. Kay, S.M. Zakeeruddin, M. Grätzel, Prog. Photovolt. 14 (2006) 589.